Journal of Mechanical Engineering and Sciences (JMES)
ISSN (Print): 2289-4659; e-ISSN: 2231-8380; Volume 1, pp. 1-15, December 2011

DOI: http://dx.doi.org/10.15282/jmes.1.2011.1.0001

EXPERIMENTAL STUDY ON HEAT TRANSFER COEFFICIENT AND FRICTION FACTOR OF Al_2O_3 NANOFLUID IN A PACKED BED COLUMN

G. Srinivasa Rao[1], K.V. Sharma[2*], S.P. Chary[3], R.A. Bakar[2], M. M. Rahman[2], K. Kadirgama[2] and M.M. Noor[4]

[1]Department of Mechanical Engineering
Kakatiya Institute of Technology and Science
Warangal, Andhra Pradesh, India,
[2]Faculty of Mechanical Engineering, Universiti Malaysia Pahang,
26600 Pekan, Pahang, Malaysia
[*]Email: kvsharma@gmail.com
[3]Andhra University, Visakhapatnam-530045, India
[4]Department of Mechanical and Mechatronic Engineering,
University of Southern Queensland, Australia

ABSTRACT

The forced convection heat transfer coefficient and friction factor are determined for the flow of water and nanofluid in a vertical packed bed column. The analysis is undertaken in the laminar and transition Reynolds number range. The column is filled with spherical glass beads as the bed material. The heat transfer coefficients with Al_2O_3 nanofluid increased by 12% to 15% with the increase of volume concentration from 0.02% to 0.5% compared with water. The experimental values of axial temperature are in good agreement with the NTU-ε method proposed by Schumann's model.

Keywords: Packed bed; Al_2O_3 nanofluid; convective heat transfer; friction factor; heat transfer enhancement.

INTRODUCTION

The process of forced convection is employed in various installations, such as boilers, solar collectors, heat exchangers, and electronic devices. However, the low thermal conductivity of heat transfer fluids, such as water, oil, and ethylene glycol mixture limits seriously improvement of their performance. To overcome this, there is need to develop advanced heat transfer fluids with significantly higher conductivity. An innovative means of improving the thermal conductivities of fluids is to suspend nano-sized solid particles in the fluid. Tuckerman and Pease (1982) conducted experiments for laminar flow in a channel. The heat transfer coefficient estimated is inversely proportional to the width of the channel, because the limiting Nusselt number is constant. Mahalingam (1985) confirmed the superiority of micro-channel cooling on a silicon substrate with a surface area of 5 × 5 cm using water and air as coolants. Many studies have been directed towards the evaluation of heat transfer coefficients for fluid flow in micro-channels.

Porous structures are also used for heat transfer augmentation as these augment the mixing of the flowing fluid and improve the convection heat transfer. Hence, studies are undertaken due to its broad applications. Early works have considered the effects of various parameters through experimental and statistical methods and have developed a

set of equations based on theoretical models for packed beds in tubular flow (Sadri, 1952).

Jeigarnik, Ivanov and Ikranikov (1991) investigated experimentally the convection heat transfer of water on flat plates and in channels packed with sintered spherical particles, nets, porous metal, and felt. The majority of the experiments is for the evaluation of heat transfer coefficients with different thickness (0.86 to 3.9 mm) and particle diameters (0.1 to 0.6 mm). They found that the porous media increased the heat transfer coefficient by 5–10 times; however, the increase in hydraulic resistance is even more. Experiments to study the percolation behavior of fluids through a packed bed were undertaken by Yagi, Kunii and Endo (1964), Gunn, Ahmad and Sabri (1987), and Lamine, Colli Serrano and Wild (1992a). Analyses of heat transfer coefficients by Weekman and Myers (1995), Silveira (1991), and Lamine, Colli Serrano and Wild (1992b) on gas-liquid flow, however, presented limited results. Adeyanju (2009) experimentally determined the velocity variations within a porous medium for packed beds. He concluded that the pressure drop across the porous medium was due to various factors, which included form drag, viscous drag from the bounding wall, and inertia force. The results from this study confirmed that the pressure drop is a linear and quadratic function of flow velocity at low and high Reynolds number, respectively. You, Moon, Jang, Kim and Koo (2010) analyzed the thermal characteristics of an N_2O catalytic igniter as a hybrid system for small satellites. The authors analyzed the problem theoretically, in order to determine the thermal performance of the catalytic igniter results on porosity, pumping capacity, and the ratio of length to diameter. Using six hydrodynamic models, Carlos, Araiza and Lopez-Isunzay (2008) predicted a generalized equation for radial velocity distribution in a packed bed with a low tube-to-particle diameter ratio. Their calculations show that the use of an effective viscosity parameter to predict experimental data could be avoided if the magnitude of the two parameters in Ergun's equation, related to viscous and inertial energy losses, are re-estimated from velocity measurements for the packed beds.

Maxwell (1904) showed the potential for increasing the thermal conductivity of a solution by mixing it with solid particles. Fluids containing small quantities of nano-sized particles are called 'nanofluids'. The particles, which are less than 100 nm in size, are dispersed uniformly within a liquid. The dispersion of nanoparticles in normal fluids enhances heat transfer, even when added in small quantities. The nanofluids show great potential for increasing heat transfer rates in a variety of cases. Lee, Choi, Li and Eastman (1999) demonstrated that CuO or Al_2O_3 nanoparticles in water and ethylene glycol exhibit enhanced thermal conductivity. The thermal conductivity increased by 20% at 4.0% concentration, when 35-nm-sized CuO nanoparticles were mixed in ethylene glycol. Mansour, Galanis and Nguyen (2007) used Al_2O_3 particles with a mean diameter of 13 nm at volume concentration of 4.3%, and reported an increase in thermal conductivity by 30%. Xuan and Roetzel (2000) presented a relation for the evaluation of the forced convection heat transfer coefficient for flow in tubes with Cu nanofluid.

Various concepts have been proposed to explain the reasons for the enhancement of heat transfer. Xuan, Li and Hu (2004) have identified two causes for the improvement of heat transfer with nanofluids: the increased dispersion due to the chaotic motion of nanoparticles that accelerates energy exchange within the fluid, and the enhanced conductivity of nanofluids considered by Choi (1995). Thermal conductivity of Al_2O_3 nanofluid has been evaluated by Das, Putra, Thiesen and Roetzel (2003) within the temperature range of 21–51 °C. They observed a two to four-fold enhancement of thermal conductivity within the range of concentration tested. Wen and

Ding (2004) evaluated the heat transfer of nanofluid in the laminar region through experiment. They used equations available in the literature to determine viscosity at bulk temperature. Maiga, Palm, Nguyen, Roy and Galanis (2005) investigated water-Al_2O_3 and Ethylene-glycol-Al_2O_3 nanofluids and observed the adverse effects of wall shear when tested with the latter. The heat transfer enhancement of nanofluids can be expected owing to intensification of turbulence, suppression of the boundary layer as well as the dispersion or back mixing of the suspended particles, a large enhancement in the surface area of nanoparticles, and a significant increase in the thermo-physical properties of the fluid. Therefore, the convective heat transfer coefficient with nanofluids is a function of the physical properties of the constituents, dimension and volume fraction of the suspended nanoparticles, and flow velocity. Sarma, Subramanyam, Kishore, Dharma Rao and Kakac (2003) and Sharma, Suryanarayana, Sarma, Rahman, Noor and Kadirgama (2010) developed a theoretical model for the estimation of the heat transfer coefficient under laminar flow in a tube with twisted tape inserts. Syam Sundar, Sharma and Ramanathan (2007) investigated heat transfer enhancement for nanofluid flow in a circular tube with twisted tape inserts.

The impact of operating parameters on heat transfer of nanofluid flow in a packed bed has not been attempted previously. The influence of nanofluid concentration on parameters affecting forced convection heat transfer in a vertical tube filled with packing materials is undertaken. The temperatures are measured at different axial positions with p-type thermocouples, as shown in Figure 1. Al_2O_3 nanofluid at 0.02%, 0.1%, and 0.5% volume concentration is pumped through the test section against gravity, both at different flow rates and at different inlet temperatures. The Nusselt number, friction factor and heat transfer coefficients are evaluated next.

Figure 1. Experimental test rig for packed bed.

MODELS FOR PREDICTING THERMAL ANALYSIS OF A PACKED BED

In order to determine the heat transfer of a packed bed system, several theoretical models have been reported in literature based on experimental investigations. A bed is of height L_B, diameter D_p and cross-sectional area 'A' and packed with material having a

void fraction 'ε', as shown in Figure 2. It is assumed that the temperature of the bed is uniform at an initial value T_{Bi}. The fluid enters at 'T_{fi}' with a mass flow rate 'm' and leaves the bed at 'T_{f0}'. The bed height L_B is divided into a certain number of elements of thickness 'Δx'. The temperature at the entry of the element is '$T_{f\,m}$' and on exit, it is at '$T_{f\,m+1}$'.

Schumann Model

Schumann (1929) has modeled the thermal behavior of packed beds, which was extended by Sagara and Nakahara (1991). The model estimates the mean fluid and solid material temperatures at a given cross section as a function of time and axial position. The assumptions made by Schumann, according to Duffie and Beckman (1991), are:

1. The bed material has infinite thermal conductivity in the radial direction with plug flow, i.e., no temperature gradient in the radial direction.
2. Bed material has zero thermal conductivity in the axial direction.
3. Thermal and physical properties of the solid and fluid are constant.
4. The heat transfer coefficient does not vary with time and position inside the bed.
5. No mass transfer occurs.
6. No heat loss to environment.
7. No phase change of the fluid in the axial direction.
8. The flow is steady and uniform.

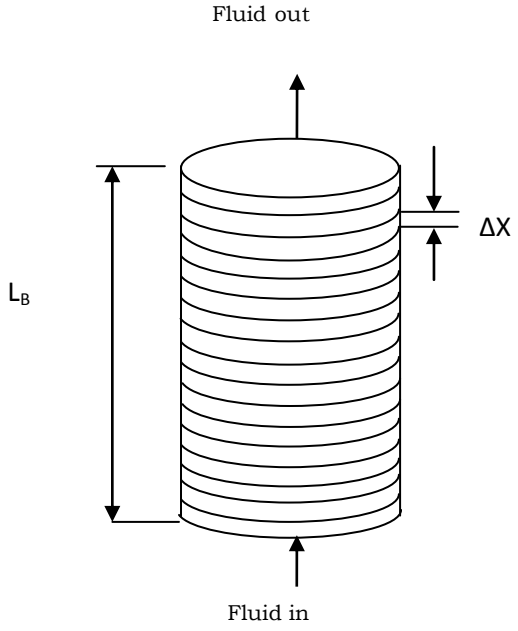

Figure 2. Elemental representation of packed bed domain.

The energy balance equation for the fluid and solid components in the Schumann model for a packed bed can be written as:

Energy in fluid at entry to bed = (Energy transferred to bed) + (Energy in the fluid in the bed) + (Energy in the fluid leaving the bed) + (Energy lost to environment)

$$m_f Cp_f T_{fi} = h_v (T_f - T_b) A dx + \rho_f C_{pf} \varepsilon A dx \frac{\partial T_f}{\partial t} + m_f C_{pf} \left(T_{fi} + \frac{\partial T_{fi}}{\partial x} dx \right) + Ul\ x (T_f - T_{fmb}) \quad (1)$$

Energy in the fluid in the bed and energy lost to the environment can be neglected as per the assumptions. Based on the assumptions stated, Eq. (1) becomes

$$\frac{\partial T_f}{\partial X} = -\frac{h_V A L_B}{\dot{m}_f C_{pf}}\left[T_f - T_S\right] \tag{2}$$

The above equation can be also written as

$$\frac{\partial T_f}{\partial X} = -\frac{h_V A L_B}{\dot{m}_f C_{pf}}\left[T_f - T_S\right] = NTU\left(T_f - T_S\right) \tag{3}$$

where $X = \frac{x}{L_B}$, NTU (Number of transfer units) = $\frac{h_V A L_B}{m_f C_{pf}}$

Energy transferred to the material = Energy stored by the material

$$h_V\left(T_f - T_s\right)A_{cs}dx = \rho_s C_{ps}(1-\varepsilon)A_{cs}dx\frac{\partial T_s}{\partial t} \tag{4}$$

The above equation can be expressed as

$$\frac{\partial T_s}{\partial \tau} = NTU(T_f - T_s) \tag{5}$$

where τ (dimensionless time) = $\frac{\dot{m}_f C_{Pf} t}{(\rho_f C_{ps})(1-\varepsilon)A_{cs}L_B)}$

Eqs. (3) and (5) give the thermal performance of the packed bed. The exit fluid temperature from the bed is obtained by integrating Eq. (3) and can be written as

$$\theta_{Th} = 1 - e^{-\frac{NTU}{N}} \tag{6}$$

The rate of heat transfer from fluid to bed element of thickness *'*Δx*'* is given by;

$$\mathrm{Q} = \dot{m}C_{pf}\left(T_{f,m+1} - T_{f,m}\right) \tag{7}$$

Eq. (7) with the aid of Eq. (6) can be written to determine the exit temperature of the fluid

$$\dot{m}C_{pf}\left(T_{f,m+1} - T_{f,m}\right) = \dot{m}_f Cp_f\left(T_{f,m} - T_{S,m}\right)\left(1 - e^{-NTU/N}\right) \tag{8}$$

Similarly, Eq. (8) can be modified to calculate the mean temperature of bed elements 'm' as given below

$$\frac{dT_{S,m}}{d\tau} = CN\left(T_{f,m} - T_{S,m}\right) \tag{9}$$

where C is a constant and equal to $1 - e^{-NTU/N}$. Eq. (9) permits energy loss to environment at temperature T_{amb} and can be written as

$$\frac{dT_{S,m}}{d\tau} = CN\left(T_{f,m} - T_{S,m}\right) + \frac{U_m \Delta A_{CS,m}}{m_f C_{Pf}}\left(T_{atm} - T_{S,m}\right) \tag{10}$$

FABRICATION OF THE EXPERIMENTAL SETUP

The experimental setup consists of a packed column 4 cm in diameter and 50-cm high. Figure 3 shows a diagram of the process and instrumentation of the experimental setup. An immersion heater heats the water, which is connected to a feed water storage tank of 50-liter capacity. A pump with flow control and bypass valves supplies a regulated flow of circulating working fluid through the test section. Suitable instrumentation is used to measure the flow rate of the working fluid, the pressure drop across the bed, and the variation of axial temperature. The working fluid flows through a helical coil immersed in the hot water tank under the action of a pump. It achieves the desired temperature before it enters the test section. The interaction between the cold bed and the hot fluid takes place. As a result, the fluid temperature at the bed outlet decreases. The fluid recirculates in a closed circuit. When the bed reaches steady state, the pressure drop

across the bed and temperatures along the bed length are obtained by personal computer through use of a data logger for glass beads of two different sizes: 6- and 14.6-mm diameter.

ESTIMATION OF PRESSURE DROP

Of interest for the flow through the packed beds is the relationship between flow velocity and the drop in pressure across the bed. Many theoretical correlations are available in the literature to calculate this. However, Sadri (1952) equation is used to calculate the pressure drop through a packed bed, given by

$$\Delta P_{Th} = \frac{150\mu V_0 L_B}{D_P^2}\frac{(1-\varepsilon)^2}{\varepsilon^3} + \frac{1.75\rho V_0^2 L_B}{D_P}\frac{(1-\varepsilon)}{\varepsilon^3} \tag{11}$$

where the bed void fraction can be determined from the relation $\varepsilon = 1 - \frac{Vol_P}{Vol_B}$, in which Vol_p and Vol_B are the volume of particles and bed, respectively, V_0 is superficial velocity, D_P is the equivalent particle diameter given by $D_P = \frac{6V_P}{S_P}$, and S_P is surface area.

The experimental pressure drop is calculated with the help of differential height in a mercury manometer given by the equation

$$\Delta P_{Exp} = R_m(\rho_A - \rho_{bf})g / g_c \tag{12}$$

The pressure drops obtained from Eq. (11) for different flow rates are compared with the experimental values and presented. The friction factors are calculated using the equation of Sadri (1952) by applying pressure drop relations and are presented as

$$f_{Ex} = \frac{\Delta P_{th} D_P}{L_B \rho_f V_S^2}\left(\frac{\varepsilon^3}{1-\varepsilon}\right) \tag{13}$$

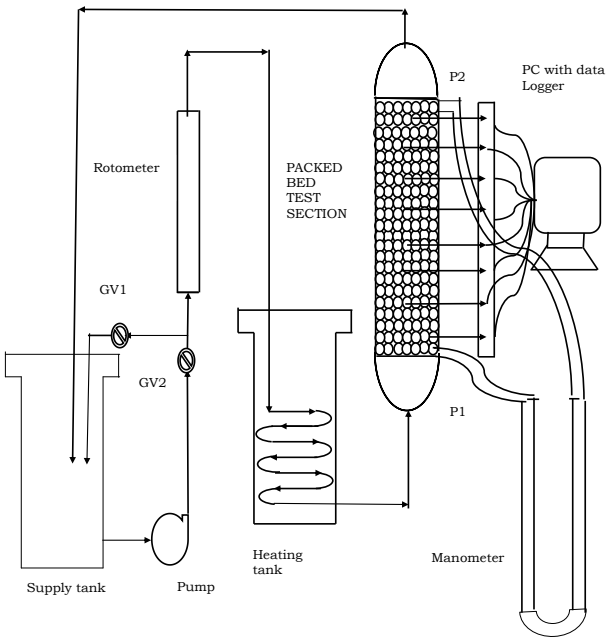

Figure 3. Schematic diagram of experiment setup of packed bed column.

CALCULATION OF HEAT TRANSFER COEFFICIENT

The energy balance equation for the packed bed can be estimated from the relation

$$Q_{Exp} = mC_{PL}(T_I - T_O) \tag{14}$$

where m is the mass flow rate. The heat transfer coefficient is estimated using Q_{Exp} and the difference between the surface temperature of the bed and the bulk mean temperature of the fluid is given by

$$h_{Exp} = \frac{Q_{Exp}}{A_S(T_S - T_{bf})} \tag{15}$$

where $\bar{T}_s = \sum_{i=1}^{i=8} T_{Si}/8$ and $T_{bf} = (T_I + T_O)/2$. The experimental Nusselt number is estimated by using the relation

$$Nu_{Exp} = \frac{h_{Exp} D_P}{k} \tag{16}$$

Alazmi and Vafai (2000) derived a correlation by conducting experiments with air, hydrogen, carbon dioxide, and water. Experiments are undertaken in a narrow range of Prandtl numbers for a packed bed Reynolds number ≤ 10000 with the characteristic dimension in Re_P taken as the bed particle diameter D_P. The validation of the correlation has been undertaken by Gnielinski (1980) who presented the relation as

$$Nu_{lam} = \frac{hD_p}{k} = 0.664 Re_p^{0.5} Pr^{1/3} \tag{17}$$

$$Nu_{tub} = \frac{hD_p}{k_f} = \frac{0.037\, Re_P^{0.8}\, P_r}{1 + 2.443\, Re_P^{-0.1}\left(P_r^{2/3} - 1\right)} \tag{18}$$

Gunn et al. (1987) presented an equation that is similar to Eq. (17) of Gnielinski (1980) in the absence of Nu_{tub} as

$$Nu = \frac{hD_p}{k} = 3.8 + 1.5\, Re_P^{0.5}\, Pr^{1/3} \tag{19}$$

Figure 4 represents the pressure drop in the packed bed with water and nanofluids at various volumetric concentrations. The pressure drop decreases with an increase in bed particle diameter and Reynolds number. The pressure drop increases with an increase in volume concentration of the nanofluid. The values of friction factor from theory are compared with those from experiment in Figure 5. The values are compared for water and nanofluid at various concentrations for 6- and 14.56-mm particles. A regression equation is developed for the estimation of friction factor with an average deviation of ±0.08% and standard deviation of 1.68% as

$$f = 20.06\, Re_p^{-0.3117}\left(1 + \varphi\right)^{0.2919} \tag{20}$$

Figures 6 to 9 represent the variation of heat transfer coefficient for various concentrations of nanofluid. Figure 6 shows the variation of heat transfer coefficient with particle Reynolds number. Nanofluids predict higher heat transfer coefficients compared with base fluid water. A regression equation is developed for the estimation of the Nusselt number as a function of the Reynolds number, Prandtl number, and volume concentration of the nanofluid. It is obtained with a standard deviation of 1.56% and an average deviation of 3.92%, as given by

$$Nu = 0.188\, Re_p^{0.98}\left(1 + \phi\right)^{0.5310} Pr^{-0.4403} \tag{21}$$

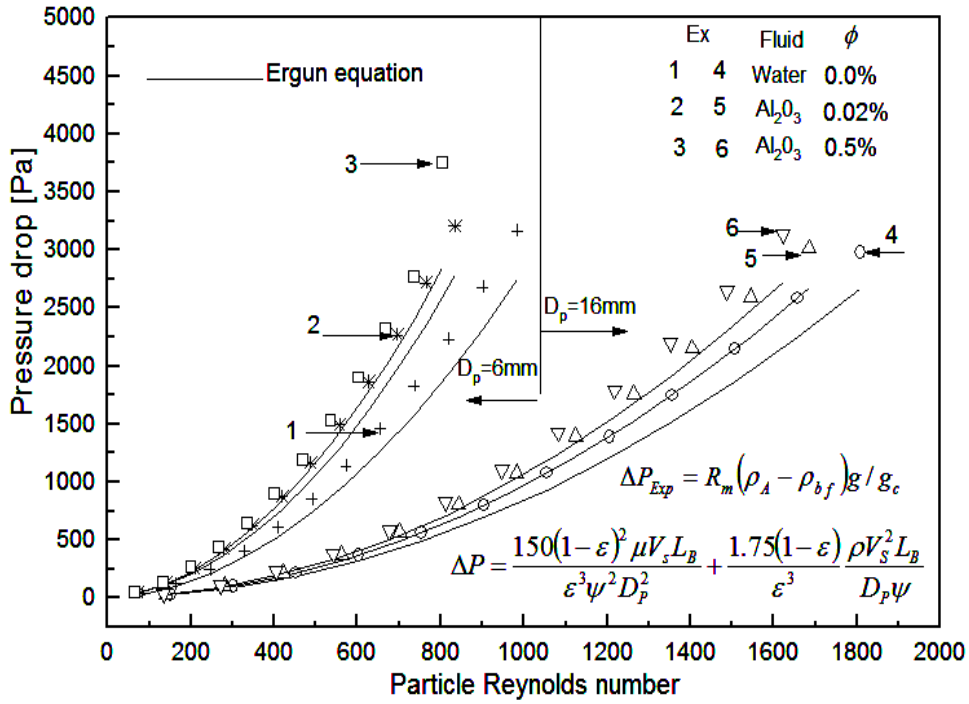

Figure 4. Comparison of experimental and theoretical pressure drop for water and nanofluids for 14.56- and 6-mm particles in packed bed.

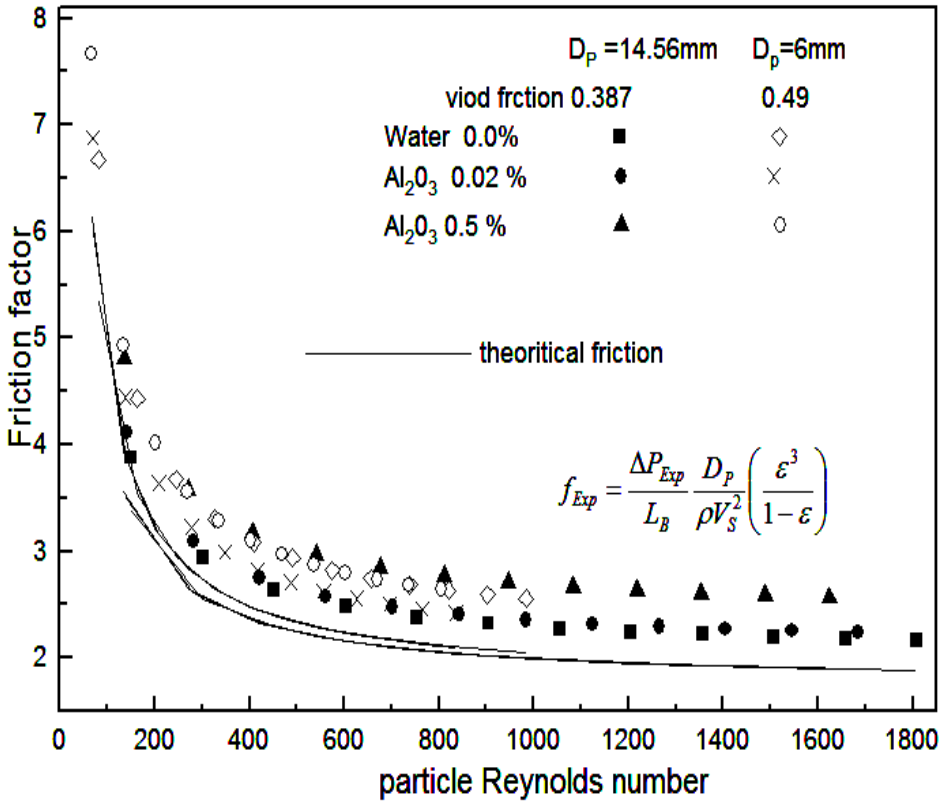

Figure 5. Comparison of experimental and theoretical friction factor for water and nanofluids for 14.56- and 6-mm particles in packed bed.

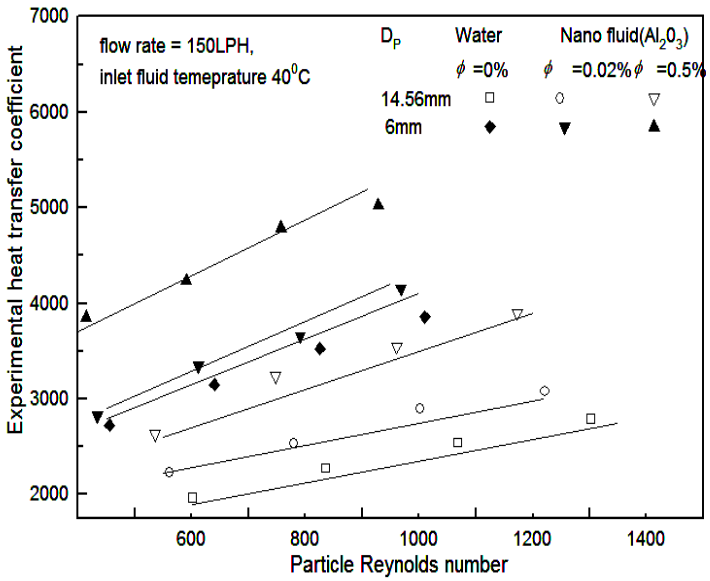

Figure 6. Comparison of heat transfer coefficient in packed beds with particle Reynolds number with 6 and 14.56 mm glass particle beds with water and nanofluids.

Figure 7 represents the variation of heat transfer coefficient with non-dimensional axial distance along the bed length at 40 °C for minimum and maximum flow rates of water and nanofluid at two different concentrations for the two particles. The heat transfer coefficient increases with increasing flow rate and concentration of the nanofluid. Figure 8 represents the variation of heat transfer coefficient for 6- and 14.56-mm particles for different operating conditions. The flow rate is 150 LPH at 40 °C for water and nanofluids at different concentration. The heat transfer coefficient increased with decreasing particle diameter.

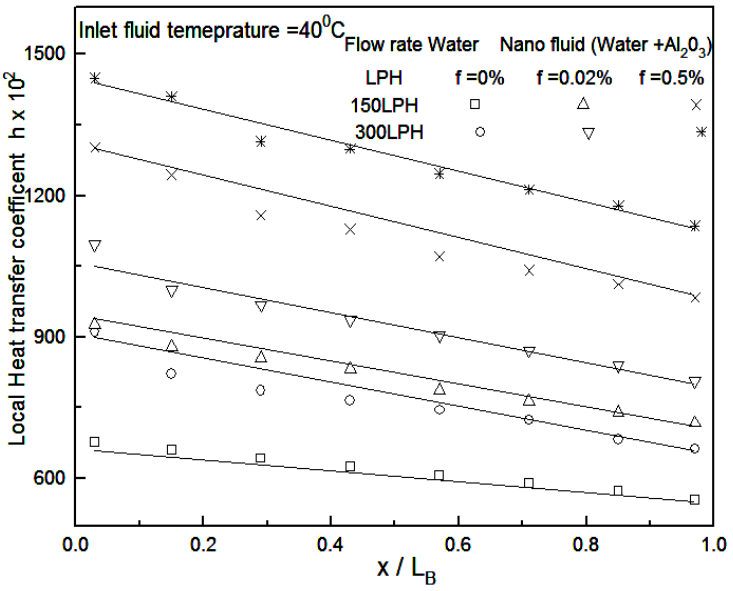

Figure 7. Effect of Al_2O_3 concentration on heat transfer coefficient comparison with non-dimensional axial distance with beds of 14.56-mm particles with water and nanofluids.

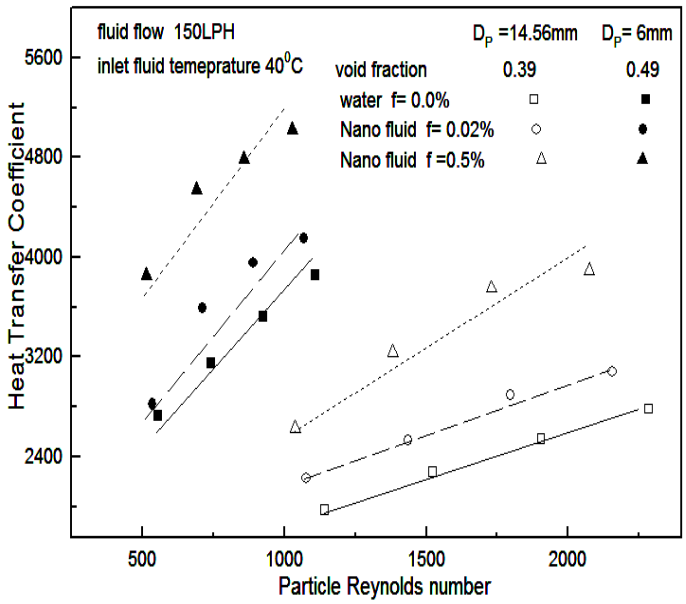

Figure 8. Heat transfer coefficient vs. particle Reynolds number at fluid rate 150 LPH for 6- and 14.56-mm particles.

Figure 9 shows the variation of heat transfer coefficient of water and nanofluid at high flow rates for two temperatures and particle concentrations. At higher flow rates and temperatures, the heat transfer coefficient is greater for 6 mm-particles compared with 14.56-mm particles.

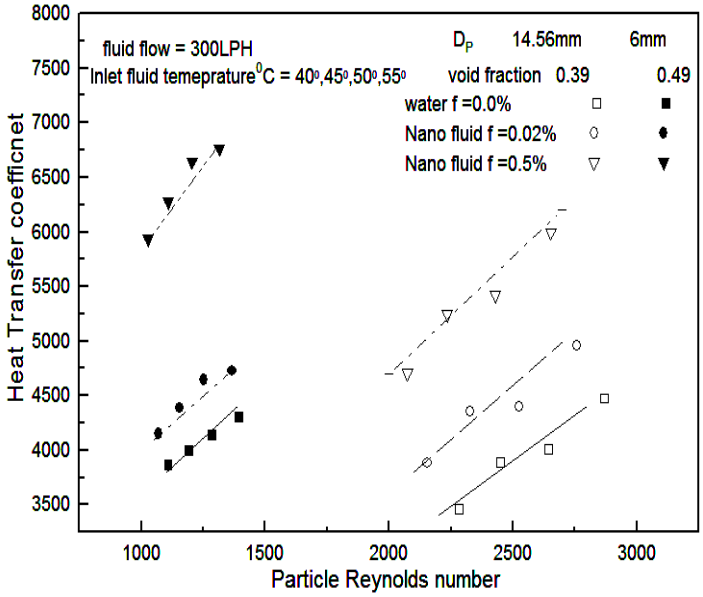

Figure 9. Heat transfer coefficient vs. particle Reynolds number at fluid rate 300 LPH for 6- and 14.56-mm particles.

Figures 10 to 11 represent the temperature distribution of the bed for two particle sizes. The experimental values are in agreement with the Schumann-NTU method and other authors from the literature. There is a reasonable agreement of

experimental data with other theoretical investigations. The pressure drop with nanofluids is higher by 10% and it increases with concentration of the nanofluid. Figure 11 shows a comparison of temperature profiles at minimum and maximum flow rate for a bed of 14.56-mm particles. At the low flow rate, the temperature is greater than at high flow rate. There is no significant temperature variation with flow rate. The temperature variation is significant at higher concentrations of the nanofluid. Figure 12 represents the non-dimensional fluid exit temperature distribution for 6-mm particles at different flow rates in comparison with the NTU method. The temperatures obtained with the nanofluid are higher than for water. The theoretical results indicate reasonable agreement with the experimental values with a deviation of 10%.

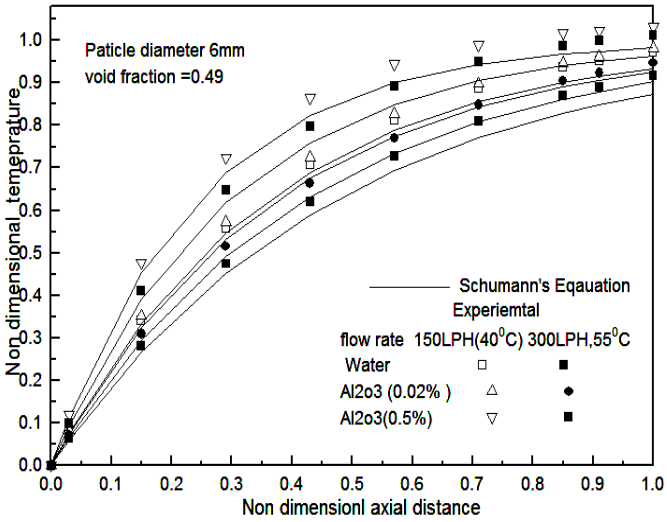

Figure 10. Comparison of non-dimensional temperature distribution with non-dimensional axial distance with NTU-ε method at 150 LPH and 300 LPH.

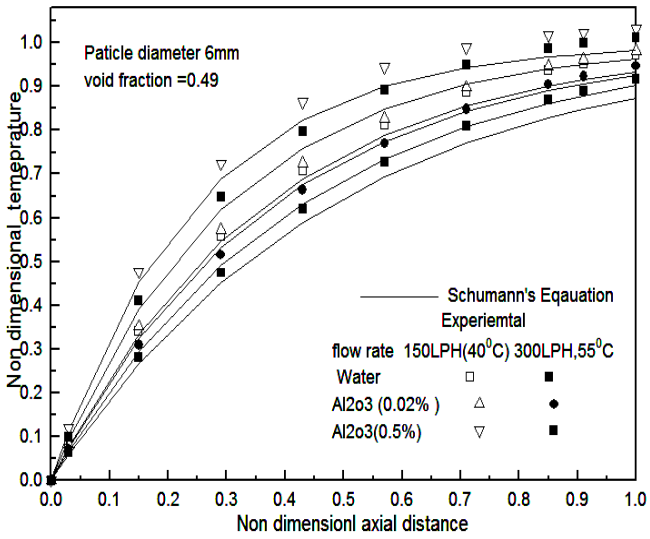

Figure 11. Comparison of non-dimensional temperature distribution with non-dimensional axial distance with NTU-ε method at 150 LPH and 300 LPH for 6-mm particles.

CONCLUSIONS

Heat transfer in a packed bed column filled with 6- and 14.56-mm-diameter glass beads, is employed to determine the heat transfer coefficient and pressure drop. The friction factor increases with decreasing particle diameter and increasing volume concentration of nanofluids compared with the base fluid. The pressure drop is higher with nanofluids than with water by 10% to 15%. The pressure drop increases with nanofluid concentration. At lower concentration, the deviation of the friction factor with nanofluid and water is more significant than at higher concentration. The heat transfer coefficient is higher with 6-mm particles owing to the larger surface area and the number of particles. Similarly, the heat transfer coefficient is greater at higher concentrations of the nanofluid. With an increase in volume concentration, the heat transfer is greater and it increases with the flow rate and inlet fluid temperature. The enhancement in heat transfer coefficient with nanofluids compared with the base fluid lies between 10% and 15% due to higher values of thermal conductivity. The values from the Schumann model agree with the experimental data for the two bead sizes of 6.0 and 14.56 mm. The deviation between the two is less than 10%.

REFERENCES

Alazmi, B., & Vafai, K. (2000). Analysis of variants within the porous media transport models. *Journal of Heat Transfer*, 122(2), 303-326.

Adeyanju, A. A. (2009). Effect of fluid flow on pressure drop in a porous medium of a packed bed. *Journal of Engineering and Applied Sciences*, 4(1), 83-86.

Araiza, C. C. O., & Isunzay, F. L. (2008). Hydrodynamic models for packed beds with low tube-to-particle diameter ratio. *International Journal of Chemical Reactor Engineering*, 6(A1), 1-8.

Carlos, O. Araiza, C., & Lopez-Isunzay, F. (2008). Hydrodynamic models for packed bedswith low tube-to-particle-diameter ratio. *International Journal of Chemical Rector Engineering*, 6(A1): 1-14.

Choi, S. U. S. (1995). Enhancing thermal conductivity of fluid with nanoparticles. Developments and applications of non-Newtonian flow. *ASME, FED* 231/MD, 66, 99-105.

Das, S. K., Putra, N., Thiesen, P., & Roetzel, W. (2003). Temperature dependence of thermal conductivity enhancement for nanofluids. *ASME Journal of Heat Transfer*, 125, 567-574.

Duffie, J. A., & Beckman, W. A. (1991). *Solar engineering of thermal processes*. 2nd ed. New York: John Wiley& Sons Inc.

Gnielinski, V. (1980). Warme- und Stoff ubertragung in Festbetten, 1980. *Chemical Engineering & Technology*, 52, 228-236.

Gunn, D. J., Ahmad, M., & Sabri, M. N. (1987). A distributed model for liquid phase heat transfer in fixed beds. *International Journal of Heat and Mass Transfe*r, 30, 1693-1702.

Jeigarnik, U. A., Ivanov, F. P., & Ikranikov, N. P. (1991). Experimental data on heat transfer and hydraulic resistance in unregulated porous structures. *Teploenergetika*, 12, 33-38.

Lamine, A. S., Colli Serrano, M. T., & Wild, G. (1992a). Hydrodynamics and heat transfer in packed beds with liquid up flow. *Chemical Engineering and Processing: Process Intensification*, 31, 385-394.

Lamine, A. S., Colli Serrano, M. T., & Wild, G. (1992b). Hydrodynamic and heat transfer packed beds with concurrent up flow. *Chemical Engineering Science*, 47, 3493-3500.

Lee, S., Choi, S. U. S., Li, S., & Eastman, J. A. (1999). Measuring thermal conductivity of fluids containing oxide nanoparticles. *Journal of Heat Transfer*, 121, 280-289.

Mahalingam, M. (1985). Thermal management in semiconductor device Packaging. *Proceedings of IEEE* 73(9), 1386-1404.

Maiga, S. B. ,Palm, S. J., Nguyen, C. T., Roy, G., & Galanis, N. (2005). Heat transfer enhancement by using nanofluids in forced convection flows. *International Journal of Heat and Fluid Flow*, 26: 530-546.

Mansour, R., Galanis, N., & Nguyen, C. (2007). Effect of uncertainties on forced convection heat transfer with nanofluids. *Applied Thermal Engineering*, 27(1), 240-249.

Maxwell, J. C. (1904). *A treatise on Electricity and magnetism*. Cambridge: Oxford University Press.

Sadri, E. (1952). Fluid flow through packed bed vertical column. *Chemical Engineering Progress*, 48: 289-294.

Sagara, K., & Nakahara, N. (1991). Thermal performance and pressure drop of rock beds with larger storage materials. *Journal of Solar Energy*, 47(3), 157-163.

Sarma. P. K., Subramanyam. T, Kishore, P. S., Dharma Rao, V., & Kakac, S. (2003). Laminar convective heat transfer with twisted tape inserts in a tube. *International Journal of Thermal Sciences*, 42(9), 821-828.

Schumann, T. E. W. (1929). Heat transfer: a liquid flowing through a porous prism. *Journal of the Franklin Institute*, 208(3), 405-416.

Sivleira, A. M. (1991). *Heat transfer in porous media one phase model in fixed beds.* Ph.D. Dissertation, PEQ-COPPE/UFRJ.

Sharma, K. V., Suryanarayana, K. V., Sarma, P. K., Rahman, M. M., Noor, M. M., & Kadirgama, K. (2010). Experimental investigations of oxygen stripping from feed water in a spray cum tray type deaerator. *International Journal of Automotive and Mechanical Engineering*, 1, 46-65.

Syam Sundar, L., Sharma, K. V., & Ramanathan, S. (2007). Experimental investigation of heat transfer enhancements with Al_2O_3 nanofluid and twisted tape insert in a circular tube. *International Journal of Nanotechnology and Applications*, 1(2), 21-28.

Tuckerman, D. B., & Pease, R. F. (1982). Ultra high thermal conductance microstructures for cooling integrated circuits. *IETE*, 781(4),145-149.

Weekman, V. W., & Myers, J. E. (1995). Heat transfer characteristics of concurrent gas-liquid flow in packed beds. *American Institute of Chemical Engineers Journal*, 11, 13-17.

Wen, D., & Ding, Y. (2004). Experimental investigation into convective heat transfer of nanofluid at the entrance region under laminar flow conditions. *International Journal of Heat and Mass Transfer*, 47(24), 5181-5188.

Xuan, Y. M., & Roetzel, W. (2000). Conceptions for heat transfer correlation of nanofluids, *International Journal of Heat and Mass Transfer*, 43(19), 3701-3707.

Xuan, Y. M., Li, Q., & Hu W. (2004). Aggregation structure and thermal conducting of nanofluids. *American Institute of Chemical Engineers Journal*, 49(4), 1038-1043.

Yagi, S., Kunii, D., & Endo, K. (1964). Heat transfer in packed beds through which water is flowing. *International Journal of Heat and Mass Transfer*, 7, 333-338.

You, W. J. Moon, H. J., Jang S. P., Kim, J. K., & Koo, J. (2010). Effects of porosity, pumping power, and L/D ratio on the thermal characteristics of an N_2O catalytic igniter with packed bed geometry. *International Journal of Heat and Mass Transfer*, 53, 726-731.

NOMENCLATURE

A	area of the bed, m^2
C	constant in Equation (9)
C_P	specific heat, J/kgK
D	diameter, m
f	friction factor
g	local acceleration of gravity, m/s^2
g_c	gravitational constant, $kg-m/N-s^2$
h	heat transfer coefficient, W/m^2K
$\bar{h}$	average heat transfer coefficient, W/m^2K
h_V	volumetric heat transfer coefficient, $W/m^{-3}K^{-1}$
k	thermal conductivity, W/mK
L	length, m
$\dot{m}$	mass flow rate, kg/s
N	number of grids in axial direction, $\Delta x/L$
NTU	Number of Transfer Units
Nu	Nusselt number, $h D_P/k$
P	pressure, Pa
ΔP	pressure drop, Pa
P_r	Prandtl number, $\mu C_{PL}/k$
Q	rate of heat transfer, W
R_e	Reynolds number, $\rho V_s D_P/\mu$
Re_p	packed bed Reynolds number, $\rho V_s D_P/\mu(1-\varepsilon)$
R_m	differential height in manometer fluid
T	temperature, K
$\bar{T}$	mean temperature, K
Vol	volume, m^3
V	velocity, m/s
X	x/L_B

Subscripts

A	mercury
B	bed
bf	bulk fluid
Ex	experimental
I	inlet

$_{lam}$	laminar flow
$_{O}$	outlet
$_{f}$	fluid
$_{L}$	liquid
$_{P}$	particle
$_{0}$	superficial
$_{S}$	surface
$_{Th}$	theoretical
$_{tub}$	turbulent flow
$_{x}$	local values
$_{Nano}$	nanofluid

Greek Symbols

θ	non-dimensional fluid temperature
ρ	density of the fluid, kg/m^3
μ	dynamic viscosity, $N-s/m$
ε	void fraction
ϕ	volume concentration